Jpn. J. Appl. Phys. Vol. 33 (1994) pp. 3602–3607
Part 1, No. 6A, June 1994

Cross Section Measurements for Electron-Impact Dissociation of CHF_3 into Neutral and Ionic Radicals

Masashi GOTO, Keiji NAKAMURA, Hirotaka TOYODA and Hideo SUGAI
Department of Electrical Engineering, Nagoya University Furo-cho, Chikusa-ku, Nagoya 464-01

(Received December 28, 1993; accepted for publication March 19, 1994)

Absolute cross sections for electron-impact dissociation of CHF_3 from the threshold to 200 eV are presented for formation of the neutral radicals CF_3, CHF_2, CF_2, CHF and CF. This measurement was accomplished by appearance mass spectrometry in a dual electron beam device. The threshold energies for neutral dissociation into CF_3, CHF_2 and CF were measured to be 11.0, 13.0 and 19.5 eV, respectively. The surface loss probability of each radical and the electron-impact nitrogen dissociation were measured to calibrate the relative dissociation cross sections of CHF_3. The branching ratio for dissociation at 150 eV is CF_3:CF_2:CF:CHF_2:CHF = 27:5:10:2:1. In addition to the neutral dissociation, the cross section for dissociative ionization of CHF_3 was extensively measured for formation of CF_3^+, CHF_2^+, CF_2^+, CHF^+, CF^+, CH^+ and F^+.

KEYWORDS: trifluoromethane, dissociation cross section, neutral radical, electron impact, ionization cross section

1. Introduction

Trifluoromethane (CHF_3) has been widely used as an etchant gas in the manufacture of semiconductors. Discharge decomposition of CHF_3 gives rise to fluorine and various neutral radicals, among which the CF_x radical ($x=1$–3) plays a key role for etching SiO_2 and for polymer growth on Si of enhancing the etch selectivity of SiO_2 to Si. Thus, a data set of electron-impact dissociation and ionization cross sections for CHF_3 is needed to understand and model the fluorine-based plasma etching system.

To date, there have been only limited data reported for CHF_3. Winters and Inokuti[1] reported the total cross section for electron-impact dissociation of CHF_3. As far as the partial cross section is concerned, Poll and Meichsner[2] measured the ionization cross section of CHF_3 into CF_3^+ and CF^+, together with the sum of cross sections into CHF_2^+ and CF_2^+. However, little information exists on cross sections for neutral dissociation, that is, electron-impact dissociation from CHF_3 into neutral radicals such as CF_3, CHF_2, CF_2, CHF and CF. This is mainly due to the difficulty in detecting neutral radicals. Recently, the authors developed a high-sensitivity radical detection technique, i.e., appearance mass spectrometry[3] which is based on the difference between the appearance potential for ionization of radicals and that for dissociative ionization of parent molecules. This technique has been successfully applied to the cross-section measurement for neutral dissociation of methane (CH_4) into CH_3 and CH_2 radicals,[4,5] and subsequently to the measurement of the dissociation cross section of carbontetrafluoride (CF_4) into CF_3, CF_2 and CF radicals,[6] as well as the cross section of tetrafluorosilane (SiF_4) into the SiF_x radical ($x=0$–3).[7]

In this paper, we report measurements of partial cross sections for electron impact dissociation of CHF_3 into neutral radicals and ionic radicals, based on the appearance mass spectrometry.

2. Experimental

Experimental measurements were made in a dual-electron-beam device combined with a quadrupole mass spectrometer (QMS), which has been used for measurements of cross sections for electron impact dissociation of methane,[4,5] carbon tetrafluoride[6] and tetrafluorosilane.[7] This system consists of three compartments which are differentially pumped with two turbomolecular pumps. The first compartment is a dissociation cell where a primary electron beam with energies of $E=5$–250 eV and currents of $I_c=0.1$–60 μA dissociates CHF_3 flowing at a pressure of 10^{-3}–10^{-2} Pa, and the electron is collected by a cylindrical cup (collector) of 1.2 cm diameter and 1.6 cm length. The second compartment is a detection cell (CHF_3 pressure: 10^{-5}–10^{-4} Pa) where a probing electron beam emitted from a rhenium filament at the energy of $E_Q=10$–25 eV selectively ionizes neutral radicals effusing from the dissociation cell through a 4-mm-diameter orifice into an ionization chamber. The ionized radicals are mass-separated by the QMS, and output pulses from a secondary electron multiplier in the QMS system are counted and processed by a computer. The third compartment is an electron source cell (CHF_3 pressure: 10^{-4}–10^{-3} Pa) where the primary electron beam is generated from a hot biased filament at the voltage $-V_d$. The primary beam is injected through a 3-mm-diameter orifice along a magnetic field of $\sim$0.06 T provided by a pair of permanent magnets, in order to minimize the beam energy spread and to define the beam trajectory.

The primary electron beam collides with CHF_3 molecules and creates various neutral radicals and ionic species. First, ions are eliminated by the positive bias ($\sim$10 eV) of the ionization chamber and the QMS with respect to the dissociation cell. Neutral radicals are detected by threshold ionization techniques[3–7] which are based on an about 5 eV difference in ionization thresholds for parent gas dissociation and radical ionization. In advance, the threshold energies for ionization of CF_x and CHF_y radicals were estimated as shown in Table I. The top column indicates the thresholds for dissociative ionization of CHF_3 which were measured in the present experiment (see §3.1). With the aid of these data, we can calculate the thresholds for radical ionization, combining a few related reactions with the following bond dissociation energies taken into ac-

Table I. Threshold energies (eV) for appearance of ions from neutral species indicated.

Neutral parent	CF_3^+	CHF_2^+	CF_2^+	CHF^+	CF^+	CH^+	F^+	Remarks
CHF_3	15.2 (H)	16.8 (F)	17.6 (HF)	19.8 (F_2)	20.9 (HF+F)	33.5 (F_2+F)	37.0	Measured (Breakup partner)
CF_3	10.6	—	18.9	—	22.2[a] 21.4[b]	—		
CHF_2		10.5	17.2	14.3	20.5[c] 14.6[d]	28.0[a] 27.2[b]		
CF_2			15.2	—	18.5	—		Expected
CHF				10.4	16.6	24.2		
CF					13.1	—		
CH						18.4		

a) and b): reactions producing 2F and F_2, respectively; c) and d): reactions producing H+F and HF, respectively.

count: $CHF_3 \rightarrow CF_3+H$, 4.6 eV; $CF_3 \rightarrow CF_2+F$, 3.7 eV; $CF_2 \rightarrow CF+F$, 5.5 eV; $CHF_3 \rightarrow CHF_2+F$, 6.3 eV; $CHF_2 \rightarrow CHF+F$, 3.9 eV; $CHF_2 \rightarrow CF_2+H$, 2.0 eV; $HF \rightarrow H+F$, 5.9 eV; $F_2 \rightarrow 2F$, 0.8 eV. In the calculation, we have selected the breakup partner to give the lower energy state in the dissociative ionization of CHF_3 as listed in Table I (see the brackets in the first column). For instance, the measured threshold of 20.9 eV for the CF^+ production was assigned to the breakup partner of (HF+F) rather than (H+2F) or (F_2+H). The expected values have an error of ~1 eV. Two different thresholds for the same CF_x^+ or CHF^+ ion from an identical neutral parent were given in the case that different fragments were produced: for example, the dissociative ionization of CHF_3 yields CF^+ with the breakup partner of 2F+H, F_2+H, or HF+F.

Figure 1 shows examples of the semilogarithmic plot of the QMS output for $m/e=69$ (CF_3^+) as a function of the energy E_Q of the probing electron beam. The energy scale of E_Q was calibrated using the measurement of the known ionization threshold (15.75 eV) of argon. For example, the CF_3^+ signal is detected as a result of the dissociative ionization $CHF_3 \rightarrow CF_3^+ + H$ above the threshold energy of 15.2 eV, and the radical ionization $CF_3 \rightarrow CF_3^+$ above the expected threshold of 10.6 eV. In Fig. 1, the output signal of CF_3^+ with the primary beam turned on (filled circles) is larger than the signal with the beam off (open circles) in the region of energies lower than 14 eV. The difference between them is attributed to electron impact ionization of CF_3 radicals effusing from the dissociation cell.

Henceforth, the probing electron energy E_Q is fixed at 13.5 eV for CF_3 detection. Let the radical signal S be the difference in the integrated QMS output between the case with the primary beam turned on and that with the beam turned off. Then, the value of S can be expressed in terms of the partial dissociation cross section $\sigma(E)$ as

$$S=\gamma I_c \sigma(E) p t, \quad (1)$$

where γ is the proportional constant, I_c and E are the current and energy of the primary beam, respectively,

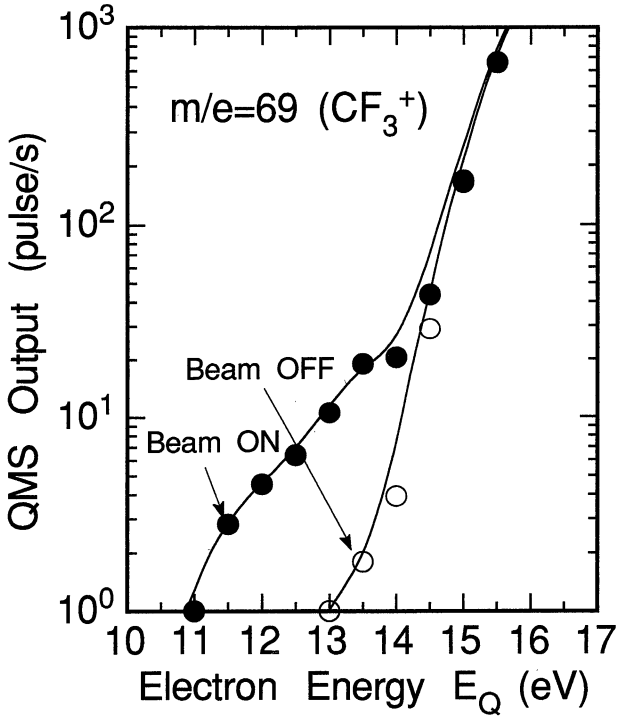

Fig. 1. Quadrupole mass spectrometer output for $m/e=69$ (CF_3^+) as a function of probing beam energy E_Q with the primary beam on (filled circles) and the primary beam off (open circles). The primary beam energy is 100 eV.

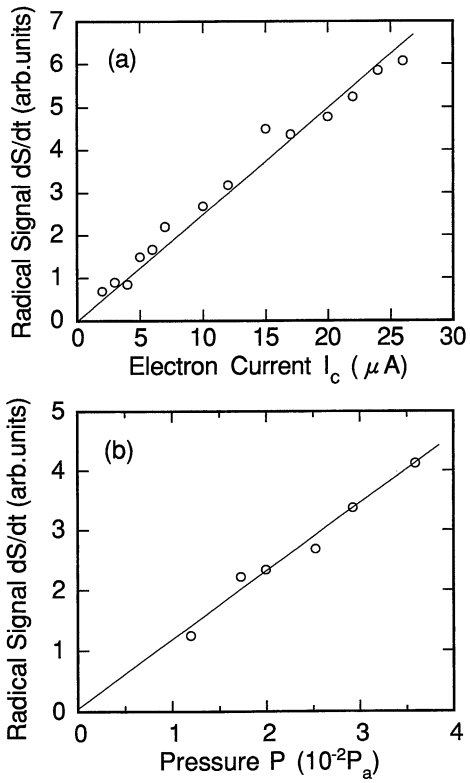

Fig. 2. (a) CHF_2 signal vs pressure at $I_c=20$ μA; (b) CHF_2 signal vs electron current at $p=1.8\times10^{-2}$ Pa; primary beam energy $E_d=80$ eV and probing beam energy $E_Q=15.5$ eV.

p is the CHF_3 pressure in the dissociation cell, and t is the integration time for pulse counting. The energy E of the primary electron beam is given by $(eV_d - e\Delta V)$,

where ΔV corresponds to the voltage drop along the hot filament. The radical signal S linearly increases with the integration time t, and the slope dS/dt of the line determined by the least squares method is proportional to the dissociation cross section.

The dependence of the CHF_2 signal (dS/dt) on the primary beam current I_c was measured as shown in Fig. 2(a). These data show that the radical signal is a linear function of electron current. Linearity was also noted with regard to the pressure dependence as shown in Fig. 2(b), and this indicates that multiple scattering processes to induce the increased path length and the decreased energy are negligible. The linearity also indicates a negligible contribution of secondary reactions which are, for instance, CF^+ formation by the secondary dissociative ionization of CF_2 produced as a result of the primary dissociation of CHF_3. The linear dependences on the electron current and the pressure were confirmed also for the species CF_2, CF, CHF_2 and CHF.

3. Results and Discussion

3.1 *Cross sections for ionization*

In order to find the threshold for ionization, the data shown on a semilogarithmic scale in Fig. 1 were replotted on a linear scale in Fig. 3. The threshold energy corresponds to the intersection of the x-axis and the straight line indicated in Fig. 3 where a small tail deviated from the straight line is caused by the energy spread ($\sim$0.5 eV) of the probing beam. Thus, the threshold energies for the dissociative ionization of CHF_3 were found as shown in the top column in Table I.

To date, the electron energy dependence of the partial cross section for dissociative ionization of CHF_3 has been reported by Poll and Meichsner[2] only for the dominant ion fragments, CF_x^+ (x=1-3), CHF_2^+, and the sum of two cross sections into CF_2^+ and CHF_2^+ without separation. To obtain information on other fragment ions, the QMS output current for m/e=32 (CHF^+), 13 (CH^+), and 19 (F^+) was also measured as a function of the probing beam energy with the primary beam turned off, as shown in Fig. 4 and Table II. The cross sections obtained here are considerably different from the previous data[2]: for instance, the cross sections at 100 eV have been reported to be 1.5×10^{-20} m^2 for CF_3^+, 3.0×10^{-20} m^2 for CF^+, and 4.0×10^{-20} m^2 for the sum of CHF_2^+ and CF_2^+. This discrepancy probably results from the different methods of calibration of the QMS sensitivity: Poll and Meichsner calibrated it with the ionization cross section of argon while we did it at

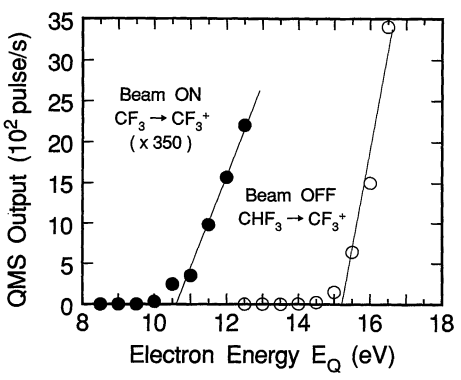

Fig. 3. Quadrupole mass spectrometer output for CF_3^+ as a function of probing beam energy E_Q with 100 eV primary beam turned on (filled circles) and off (open circles).

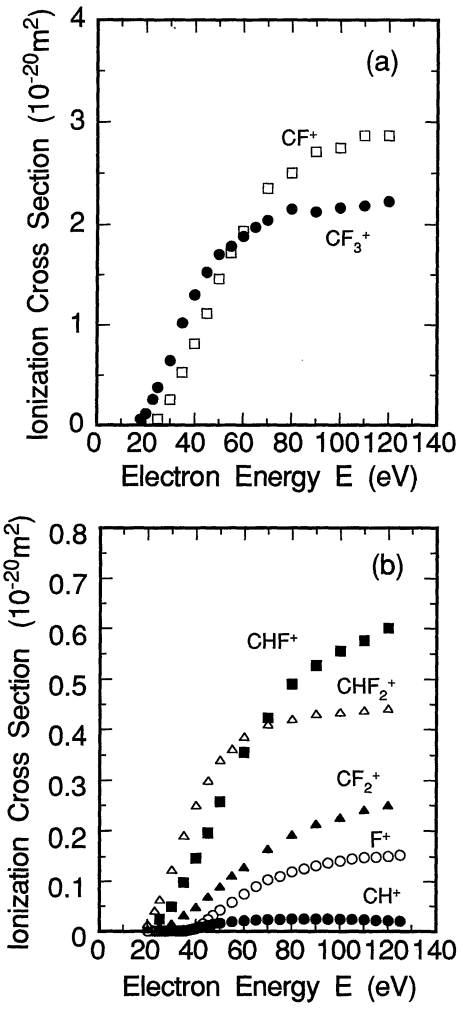

Fig. 4. Partial cross sections for ionization (a) $CHF_3 \rightarrow CF_3^+$ and CF^+, and (b) $CHF_3^+ \rightarrow CHF_2^+$, CF_2^+, CHF^+, CH^+ and F^+.

Table II. Cross section for dissociative ionization of CHF_3 in units of 10^{-20} m^2.

Energy (eV)	CF_3^+	CHF_2^+	CF_2^+	CHF^+	CF^+	CH^+	F^+
20	0.115	0.014	0.004				
25	0.381	0.064	0.009	0.025	0.061		
30	0.641	0.124	0.016	0.049	0.257		
35	1.02	0.191	0.033	0.098	0.527	0.001	0.001
40	1.30	0.250	0.048	0.147	0.809	0.005	0.006
45	1.52	0.300	0.069	0.196	1.12	0.012	0.023
50	1.70	0.341	0.090	0.257	1.46	0.017	0.043
60	1.88	0.386	0.129	0.355	1.94	0.021	0.074
70	2.04	0.410	0.166	0.422	2.35	0.023	0.104
80	2.15	0.421	0.193	0.490	2.50	0.025	0.119
90	2.12	0.431	0.214	0.527	2.71	0.025	0.132
100	2.16	0.434	0.226	0.555	2.75	0.024	0.142
110	2.18	0.438	0.241	0.576	2.87	0.023	0.148
120	2.22	0.441	0.250	0.600	2.88	0.021	0.151

each mass of CF_x^+ ($x=1$–3) compared with the ionization cross section of CF_4,[8] thus taking account of mass discrimination effects of the QMS. The QMS sensitivity for CH^+ was calibrated by measuring the CH^+ production from ionization of CH_4 compared with the known cross section,[9] while the sensitivities for CHF_2^+ and CHF^+ were assumed to be equal to those for CF_2^+ and CF^+, respectively.

3.2 *Cross sections for neutral dissociation*

The threshold for appearance of neutral radicals as a result of dissociation of CHF_3 has never been measured, to our knowledge. In addition, it cannot be estimated by calculation, even using all the known data in Table I. For such calculations, we need at least one additional experimental datum on the threshold for electron-impact neutral dissociation, *e.g.*, for $CHF_3+e\rightarrow CHF_2+F+e$. To obtain such data, the dependence of the neutral radical signal on the primary beam energy E was measured, especially for low energies, as shown in Fig. 5. According to these measurements, the threshold energies for neutral dissociation were obtained with errors of ~1 eV and summarized in the right-most column in Table III. If the thresholds for CF_3 and CHF_2 appearance are correct, i.e. 11.0 eV and 13.0 eV, respectively, then the thresholds for CF_2, CF and CHF production can easily be calculated using the dissociation energies for CF_2-F, CF-F, CF_2-H, CHF-F, H-F and F-F bonds. These expected values are listed in Table III and a comparison with the measured values suggests that the observed threshold corresponds to the reaction yielding F_2+H [Reaction (8)]

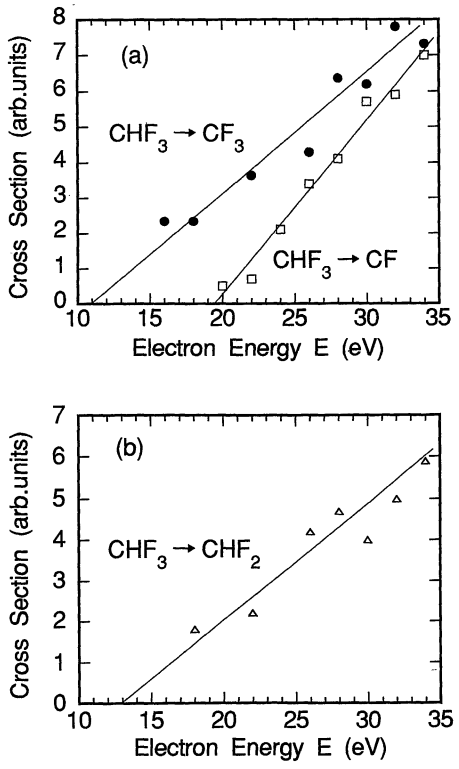

Fig. 5. Relative cross sections near the threshold for neutral dissociation of CHF_3 into (a) CF_3 (filled circles) and CF (open squares), and (b) CHF_2.

Table III. Threshold energies for neutral dissociation.

Number	Reaction	Threshold energy (eV) Expected[a]	Measured[b]
(1)	$CHF_3+e\rightarrow CF_3+H+e$	11.0	11.0
(2)	$CHF_3+e\rightarrow CHF_2+H+e$	13.0	13.0
(3)	$CHF_3+e\rightarrow CF_2+H+F+e$	15.0	<25
(4)	$CHF_3+e\rightarrow CF_2+HF+e$	9.1	
(5)	$CHF_3+e\rightarrow CHF+2F+e$	16.9	<37
(6)	$CHF_3+e\rightarrow CHF+F_2+e$	16.1	
(7)	$CHF_3+e\rightarrow CF+H+2F+e$	20.5	
(8)	$CHF_3+e\rightarrow CF+F_2+H+e$	19.7	19.5
(9)	$CHF_3+e\rightarrow CF+HF+F+e$	14.6	

[a] Threshold energies 11.0 eV and 13.0 eV were assumed for reactions (1) and (2), respectively.
[b] Experimental error was about ±0.5 eV.

rather than H+2F or HF+F [Reaction (7) or (9), Table III]. It should be noted that the threshold for dissociation into F^+ and CF_x or CHF_y is higher, by the ionization energy of 17.4 eV ($F\rightarrow F^+$), than the threshold for neutral dissociation into F and CF_x or CHF_y.

The absolute value of cross sections was determined using the same method as noted previously.[5-7] Let us take an example of the CF_3 radical and summarize the calibration process briefly. The partial cross section σ for dissociation from CHF_3 to CF_3 can be expressed as

$$\sigma=\frac{\alpha}{\beta\sigma^*[CHF_3]}\cdot\frac{dS}{dt}, \tag{2}$$

where σ^* denotes the ionization cross section for $CF_3\rightarrow CF_3^+$, $[CHF_3]$ is the number density of CHF_3 molecules in the dissociation cell, and $\beta=ll'I_cI'/e^2$ for the electron path lengths l and l', and the currents I_c and I', in the dissociation cell and the detection cell, respectively. The proportional constant α depends on the vacuum conductances, C_a and C_b, of two orifices through which the radical effuses out of the dissociation cell. The value of α also depends on the loss rate $k=svA/4$ due to the radical surface loss on the dissociation cell wall of the area A, where s denotes the surface loss probability and v is the thermal speed of the radical. Taking account of these factors, we obtain the final expression[5] for the cross section

$$\alpha=\frac{\mu\gamma\, k+C_a+C_b}{\beta\,\sigma^*[CHF_3]C_a}\cdot\frac{dS}{dt}, \tag{3}$$

where γ is the constant independent of radical species and μ denotes the constant expressing the mass discrimination effect of QMS. The vacuum conductances for CF_3 are found to be $C_a=0.49\ l\ s^{-1}$ and $C_b=0.28\ l\ s^{-1}$. The conductances for each radical can be calculated with its mass dependence taken into account as shown in Table IV.

The surface loss rate k can be obtained by measuring the time decay of radical density after turning off the primary electron beam. The radical density exponentially decreases with the time constant $\tau=V/(k+C_a+C_b)$ for the volume V of the dissociation cell. The observed density decay of CF_3, CF_2, CF, CHF_2 and CHF is shown in Fig. 6, together with the data

Table IV. Decay time constant τ, vacuum conductances C_a and C_b, surface loss rate k, and surface loss probability s for dissociation products N, CF_3, CHF_2, CF_2, CHF and CF.

Product	τ (ms)	C_a ($l\,s^{-1}$)	C_b ($l\,s^{-1}$)	k ($l\,s^{-1}$)	s
N	0.80	1.09	0.62	17.0	0.014
CF_3	0.48	0.49	0.28	30.5	0.056
CF_2	0.42	0.58	0.33	34.8	0.055
CF	0.22	0.73	0.42	67.0	0.083
CHF_2	0.80	0.57	0.32	17.9	0.028
CHF	0.74	0.72	0.41	19.1	0.024

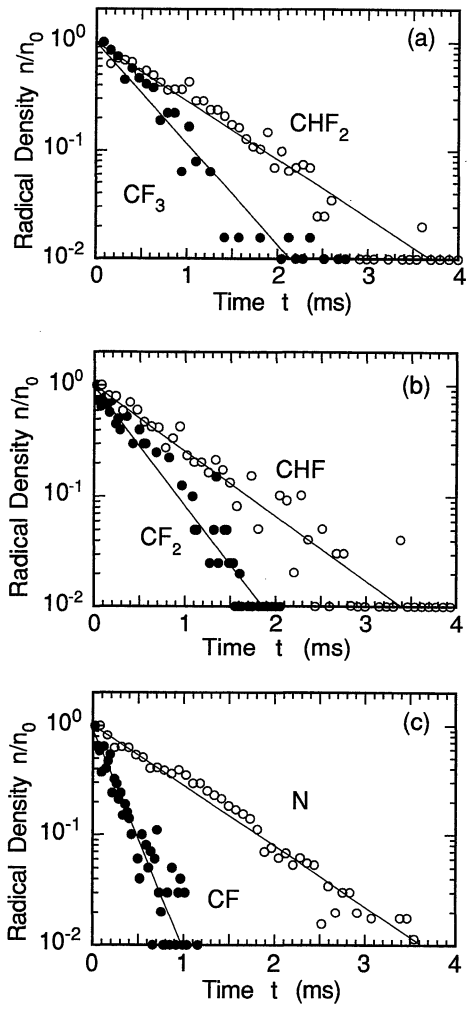

Fig. 6. Density decay after turning off the primary electron beam for (a) CF_3 radical (filled circles) and CHF_2 radical (open circles); (b) CF_2 radical (filled circles) and CHF radical (open circles); (c) CF radical (filled circles) and N atom (open circles).

for the N atom used for calibration.[5] Table IV shows the measured time constant τ, the surface loss rate k, and the surface loss probability s where the volume $V=15$ cm^3, the surface area $A=62$ cm^2, and the radical speed $v=(8kT/\pi m)^{1/2}$ at $T=400$ K were used. The time constants obtained for CF_3, CF_2, CF and N are smaller than the results previously obtained in the experiment for CF_4 dissociation.[6] This discrepancy may result from different wall surfaces (H-containing surface layer) due to CHF_3 dissociation, and partly from the higher temperature of walls due to the reconstructed filament system of the electron source cell.

Neglecting the mass dependence of QMS sensitivity, the proportional constant γ in eq. (3) can be obtained, just as in the previous study on methane,[5] by measurements of electron impact dissociation $N_2 \rightarrow N+N$, $N+N^+$ and a comparison of them with the known cross section of nitrogen. On the other hand, the proportional constant μ, i.e., the mass discrimination effect of QMS was carefully calibrated as follows. With the primary electron beam turned off, CHF_3 or N_2 molecules were ionized by the probing electron beam and the resultant fragment ion CF_3^+ or N^+ was detected by QMS. The measured energy dependence of CF_3^+ or N^+ signal was compared with the known absolute cross sections,[8,10] which gives the ratio of μ values. Thus, the conversion factor to obtain the absolute cross section from our raw data was found to be $CF_3^+:CHF_2^+:CF_2^+:CHF^+:CF^+:N^+=3.4:1:1:4.0:4.0:2.1$, assuming the same values of μ for CHF_2^+ as CF_2^+ and for CHF^+ as CF^+. Finally, we need the ionization cross section σ^* of radical species to obtain the absolute value according to eq. (3). The cross sections for $CF_3 \rightarrow CF_3^+$ have been measured as functions of electron energy E by Wetzel *et al.*[11] but there are no data for $CF_x \rightarrow CF_x^+$ or $CHF_x \rightarrow CHF_x^+$ ($x=1$, 2). There are a few examples of ionization cross sections for the neutral free radicals CD_2 and SiF_2, which have the same slope ($\Delta\sigma/\Delta E \sim 1.1\times10^{-21}$ m^2 eV^{-1}) as the CD_3 and SiF_3, respectively.[12-14] Thus, we tentatively assumed that the ionization cross sections for CF_2, CF, CHF_2 and CHF increase from their thresholds with the same slope ($\Delta\sigma/\Delta E \sim 3.3\times10^{-22}$ m^2 eV^{-1}) as the CF_3 ionization cross section.

The absolute values of partial cross sections for dissociation of CHF_3 into CF_3, CF_2, CF, CHF_2 and CHF radicals are shown in Fig. 7 and Table V. We estimate that the absolute uncertainty of the cross section is $\pm100\%$ and the relative uncertainty is $\pm20\%$, as discussed previously.[5] The cross sections for CF, CF_2 and CF_3 have maxima at $E=40$, 70 and 110 eV, respectively and gently decrease. Thus, the energy at the maximum becomes smaller for smaller fragments. This behavior is similar to the energy dependence of partial cross sections for dissociation of CF_4 into neutral radicals.[6] This figure shows an interesting tendency that the energy at the maximum becomes smaller for smaller fragments. The branching ratio at $E=150$ eV was $CF_3:CF_2:CF:CHF_2:CHF=27:5:10:2:1$. In contrast with these results, electron impact neutral dissociation of methane[4,5] has a maximum cross section at low energies (20–25 eV), and the branching ratio between CH_3 and CH_2 strongly depends on the impact energy, since the CH_2 radical is resonantly produced in a range of energy between 10 eV and 40 eV.

The total dissociation cross section σ_t of CHF_3 has been reported by Winters and Inokuti[1] as $\sigma_t=2.4\times10^{-20}$ m^2 at $E=22$ eV, 5.5×10^{-20} m^2 at 72 eV and 5.8×10^{-20} m^2 at 100 eV. The present investigation on the partial cross section of CHF_3 enables us to estimate the total cross section by summing up each cross

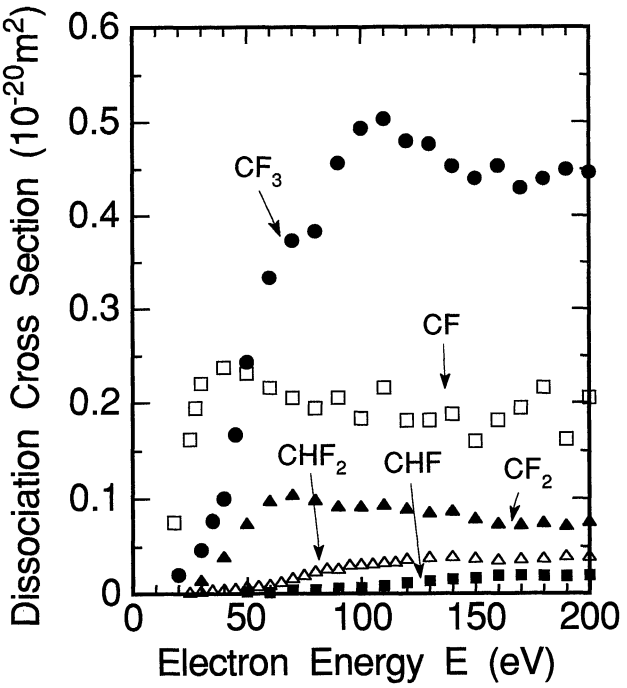

Fig. 7. Absolute cross sections for neutral dissociation of CHF_3 into CF_3 (filled circles), CHF_2 (open triangles), CF_2 (filled triangles), CHF (filled squares) and CF (open squares).

Table V. Cross section for dissociation of CHF_3 into neutral fragments in units of 10^{-20} m^2.

Energy (eV)	CF_3	CHF_2	CF_2	CHF	CF
20	0.02	0.001			0.01
25	0.03	0.002			0.16
30	0.05	0.003	0.014		0.22
35	0.08	0.004	0.025		0.23
40	0.10	0.005	0.040		0.24
50	0.24	0.008	0.075	0.002	0.23
60	0.33	0.010	0.098	0.002	0.22
70	0.37	0.017	0.104	0.004	0.21
80	0.38	0.024	0.099	0.004	0.19
90	0.46	0.027	0.092	0.005	0.20
100	0.49	0.032	0.092	0.006	0.18
110	0.50	0.034	0.094	0.008	0.21
120	0.48	0.038	0.090	0.011	0.18
130	0.47	0.039	0.086	0.014	0.18
140	0.45	0.040	0.088	0.015	0.19
150	0.44	0.038	0.080	0.016	0.16
160	0.45	0.037	0.075	0.019	0.18
170	0.43	0.038	0.074	0.019	0.19
180	0.44	0.038	0.076	0.019	0.20
190	0.45	0.041	0.073	0.018	0.16
200	0.44	0.040	0.076	0.019	0.20

section for the ionization (Table II) and the neutral dissociation (Table V). For example, we obtain $\sigma_t = 0.17 \times 10^{-20}$ m^2 at $E = 20$ eV, 6.2×10^{-20} m^2 at 70 eV, and 7.1×10^{-20} m^2 at 100 eV. These results roughly agree with Winters's report[1] except for the lower energies.

4. Conclusions

Earlier studies on electron CHF_3 collisons were limited to the total dissociation cross section[1] and the partial ionization cross sections for parent $CHF_3 \rightarrow CF_3^+$, CF^+, with the sum of CF_2^+ and CHF_2^+. This paper reports the extensive measurements of cross sections for (1) the dissociative ionization $CHF_3 \rightarrow CF_x^+$ ($x=1$-3), CHF_y^+ ($y=1$, 2), CH^+ and F^+ and (2) the neutral dissociation $CHF_3 \rightarrow CF_x$ ($x=1$-3) and CHF_y ($y=1$, 2). The threshold energies for neutral dissociation into CF_3, CHF_2 and CF were found, for the first time, to be 11.0 eV, 13.0 eV and 19.5 eV, respectively. The absolute cross section for dissociation into neutral radicals was measured as a function of electron energy from the threshold to 200 eV and the absolute value of the cross section was determined using the procedure described previously.[5-7] The branching ratio at the electron energy of 150 eV is CF_3:CF_2:CF:CHF_2:CHF = 27:5:10:2:1.

Acknowlegements

This work was carried out partly under the collaborating Research Program at the National Institute for Fusion Science, and was partly supported by a Grant-in-Aid for Scientific Research from the Ministry of Education, Science and Culture.

1) H. F. Winters and M. Inokuti: Phys. Rev. A **25** (1982) 1420.
2) H. U. Poll and J. Meichsner: Contrib. Plasma Phys. **27** (1987) 359.
3) H. Sugai and H. Toyoda: J. Vac. Sci. & Technol. A **10** (1992) 1193.
4) T. Nakano, H. Toyoda and H. Sugai: Jpn. J. Appl. Phys. **30** (1991) 2908.
5) T. Nakano, H. Toyoda and H. Sugai: Jpn. J. Appl. Phys. **30** (1991) 2912.
6) T. Nakano and H. Sugai: Jpn. J. Appl. Phys. **32** (1992) 2919.
7) T. Nakano and H. Sugai: J. Phys. D **26** (1993) 1909.
8) Ce Ma, M. R. Bruce and R. A. Bonham: Phys. Rev. A **44** (1991) 2921.
9) H. Chatham, D. Hils, R. Robertson and A. Gallagher: J. Chem. Phys. **81** (1984) 1770.
10) D. Rapp and P. Englander-Golden: J. Chem. Phys. **43** (1965) 1464.
11) R. C. Wetzel, F. A. Baiocchi and R. S. Freund: Abstr. 37th Gaseous Electronics Conf. (Boulder, Colorado, 1984).
12) F. A. Baiocchi, R. C. Wetzel and R. S. Freund: Phys. Rev. Lett. **53** (1984) 771.
13) T. R. Hayes, R. J. Shul, F. A. Balocchi, R. C. Wetzel and R. S. Freund: J. Chem. Phys. **89** (1988) 4035.
14) R. J. Shul, T. R. Hayes, R. C. Wetzel, F. A. Baiocchi and R. S. Freund: J. Chem. Phys. **89** (1988) 4042.